Contribution from the Department of Chemistry, West Virginia University, Morgantown, West Virginia 26506, Chemistry Division, Argonne National Laboratory, Argonne, Illinois 60439, and Department of Chemistry, Brookhaven National Laboratory, Upton, New York 11973

Low-Temperature (20 K) Neutron Diffraction Study of [K(crypt-222)]+[Cr2(CO)10(μ-H)]−. Influence of the Lattice Environment and the K+ Ion on the Anion's Metal Carbonyl Framework and the Ordered Cr–H–Cr Bond[1]

JEFFREY L. PETERSEN,*[2a] RICHARD K. BROWN,[2b,c] and JACK M. WILLIAMS*[2b]

A combination room-temperature X-ray and low-temperature (20 ± 1 K) neutron diffraction study of [K-(C18H36N2O6)]+[Cr2(CO)10(μ-H)]− has been performed to determine the anion's configuration in the absence of crystallographic site symmetry constraints. Although the K+ ion is surrounded by the cryptate molecule, the ion influences the anion's solid-state structure. The relatively close separation of 2.966 (3) Å between the K+ ion and O1 of the anion is nearly equal to the sum of the corresponding ionic radii of ca. 2.9 Å and thereby suggests the presence of an appreciable cation–anion interaction. Although this attractive interaction does not noticeably perturb the local C_{4v} symmetry of the respective Cr(CO)5 fragment, it causes the anion's eclipsed metal carbonyl structure to undergo a twisting distortion toward a previously unobserved bent structure. The two independent Cr(CO)5 groups of the anion are rotated ca. 19° with respect to each other about the Cr–Cr line. This configurational change in the metal carbonyl framework is accompanied by a reduction of the Cr⋯Cr separation to 3.300 (4) Å and the Cr–H–Cr bond angle to 145.2 (3)°, which collectively imply an increase in the metal–metal bonding component of the closed three-center, two-electron Cr–H–Cr bond. The ordered bridging hydrogen atom resides in a symmetrical electronic environment as suggested by the two independent, but equivalent, Cr–H separations of 1.735 (5) and 1.723 (5) Å. These Cr–H distances are comparable in magnitude to the corresponding distances in the [Et4N]+ and [(Ph3P)2N]+ salts. The neutron-determined lattice parameters for the monoclinic cell, $P2_1/c$, are a = 10.461 (4) Å, b = 14.416 (7) Å, c = 23.863 (7) Å, and β = 97.24 (4)°, for λ 1.1173 (2) Å. Block-diagonal least-squares refinements (based on F_o) converged with discrepancy indices of $R(F_o)$ = 0.039 and $R_w(F_o)$ = 0.032 with σ_1 = 1.06 for 4444 reflections with F_o > 0. The neutron diffraction data were measured with an automated four-circle diffractometer at the Brookhaven high-flux beam reactor.

Introduction

Structural studies of the molecular configuration of the [M2(CO)10(μ-H)]− monoanion, where M = Cr,[3] Mo,[4] and W,[5] have shown that its solid-state geometry is dependent, because of the flexible nature of the M–H–M linkage, upon the lattice packing forces. Two principal geometries have been observed. For the [(Ph3P)2N]+ salts of the Mo[4] and W[5] analogues, a bent, staggered carbonyl configuration exists, whereas for the [Et4N]+ and [(Ph3P)2N]+ salts[3] of the dichromium anion a linear, eclipsed metal carbonyl framework is found. However, for these latter salts, the anion's geometry is constrained by a crystallographic center of inversion. Another result of this constraint is that the μ-H atom's position is disordered among sites displaced ca. 0.3 Å from the Cr–Cr bond line. Consequently, we have prepared the [K(C18H36N2O6)]+ or [K-(crypt-222)]+ salt of the [Cr2(CO)10(μ-H)]− monoanion in an attempt to remove both the imposed site symmetry and the accompanying crystallographic disorder. The [K(crypt-222)]+ cation was selected because of its chirality which might reduce the site symmetry previously observed for the anion[3] and because of the preference for complexation of the K+ ion by this cryptate molecule. Our immediate goal was to determine if the [Cr2(CO)10(μ-H)]− anion prefers, in the absence of crystallographic site symmetry, a slightly bent structure with one

off-axis μ-H atom position or a D_{4h} structure accompanied by a fourfold disorder of the μ-H atom configuration. The outcome of our X-ray (293 K) and neutron diffraction (20 K) analyses has provided the first clear evidence of the cation's influence upon the anion's solid-state geometry. Collectively, our efforts have provided detailed structural information about the nature of the metal–hydrogen interaction in the [Cr2-(CO)10(μ-H)]− anion and have demonstrated the extent to which packing effects and cation–anion interactions influence the anion's structure.

Experimental Section

The borohydride reduction of Cr(CO)6 was carried out by using Schlenk glassware under a dry-nitrogen atmosphere. Sodium benzophenone ketyl was employed to dry and scavenge O2 from the solvents during their distillation under N2 or Ar prior to use. Cr(CO)6 was purchased from Strem Chemical Co. and KBH4 and crypt-222, C18H36N2O6, were obtained from PCR, Inc. The infrared spectra were recorded on a Beckman IR-8 spectrometer. Proton NMR spectra (CDCl3) were measured on a Varian CFT-20 spectrometer operating in the FT mode.

Preparation of [K(crypt-222)]+[Cr2(CO)10(μ-H)]−. The [K-(crypt-222)]+ salt was prepared by a modification of published methods.[6] To a Schlenk tube containing 1.2 g (5.5 mmol) of Cr(CO)6 and 0.2 g (3.5 mmol) of KBH4 was added about 50 mL of freshly distilled THF. The mixture was refluxed for 24 h and filtered; the solvent was removed in vacuo. Then 25 mL of a degassed absolute ethanol solution containing 1 g (2.7 mmol) of crypt-222 were added. Upon cooling of the solution a yellow solid product separated and was isolated upon filtration to yield 1.6 g (2.0 mmol) of crude product. The analytical sample was recrystallized from THF/hexane or ethanol. Anal. Calcd for C28H37N2O16KCr2: C, 42.00; H, 4.66. Found: C, 42.01; H, 4.70. IR (CH2Cl2): ν(CO) 2033 (w), 1942 (vs), 1875 (s) cm−1. 1H NMR (cation): τ 7.46 (CH2N, t, J_{H-H} = 6 Hz), 6.47 (CH2O, t, J_{H-H} = 6 Hz), 6.41 (OCH2CH2O, s). Suitable crystals for the structural analyses were grown by slow cooling of a saturated ethanol solution of the salt.

X-ray Diffraction Data Collection and Structural Analysis. A parallelepiped-shaped crystal of [K(crypt-222)]+[Cr2(CO)10(μ-H)]−

(1) This work was performed under the auspices of the Division of Basic Energy Sciences of the U.S. Department of Energy.
(2) (a) West Virginia University. (b) Argonne National Laboratory. (c) Research collaborator at Brookhaven National Laboratory from Argonne National Laboratory.
(3) (a) Roziere, J.; Williams, J. M.; Stewart, R. P., Jr.; Petersen, J. L.; Dahl, L. F. *J. Am. Chem. Soc.* 1977, 99, 4497. (b) Petersen, J. L.; Johnson, P. L.; O'Connor, J.; Dahl, L. F.; Williams, J. M. *Inorg. Chem.* 1978, 17, 3460. (c) Petersen, J. L.; Brown, R. K.; Williams, J. M.; McMullan, R. K. *Ibid.* 1979, 18, 3493.
(4) Petersen, J. L.; Masino, A.; Stewart, R. P., Jr.; submitted for publication.
(5) (a) Wilson, R. D.; Graham, S. A.; Bau, R. *J. Organomet. Chem.* 1975, 91, C49. (b) Hart, D.; Bau, R.; Koetzle, T., manuscript in preparation. (c) Bau, R.; Teller, R. G.; Kirtley, S. W.; Koetzle, T. F. *Acc. Chem. Res.* 1979, 12, 176 and references cited therein.
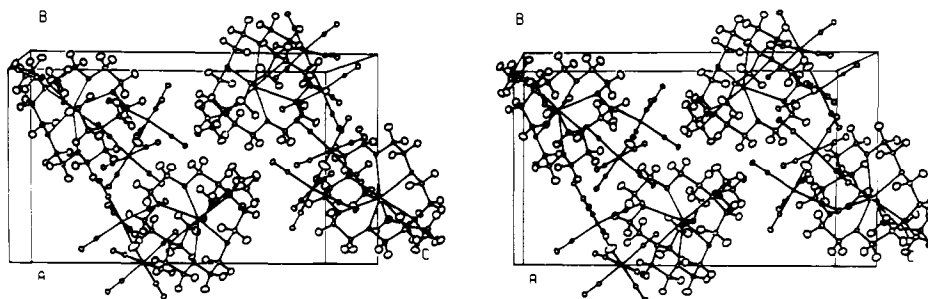(6) Hayter, R. G. *J. Am. Chem. Soc.* 1966, 88, 4376.

Figure 1. Stereographic illustration of the molecular arrangement of the four $[K(crypt-222)]^+$ cations and four $[Cr_2(CO)_{10}(\mu\text{-H})]^-$ anions in the monoclinic unit cell. The thermal ellipsoids of nuclear motion for all the atoms in this and subsequent drawings are scaled to enclose 50% probability. Notice that one of the anion's carbonyl groups is directed toward the K^+ ion in the cation.

was mounted with the a axis nearly parallel to the spindle axis of the goniometer. Inspection of the oscillation and Weissenberg photographs taken with Cu Kα radiation revealed the space group to be monoclinic, $P2_1/c$ (C_{2h}^5, No. 14). The sample was transferred to a Picker full-circle goniostat which operates under computer control with use of a Krisel control diffractometer automation package. The angular coordinates (ω, χ, 2θ) for 20 diffraction peaks with $15° < 2\theta < 25°$ were automatically centered; least-squares refinement yielded the corresponding lattice parameters given in Table I. The experimental density of 1.41 g/cm³ was determined by flotation in a CCl₄/toluene solution.

Intensity data (hkl, $\bar{h}kl$) were measured with Zr-filtered Mo Kα X-ray radiation at a takeoff angle of 2° within a detector range of $3° \leq 2\theta \leq 40°$. The θ–2θ scan mode was employed to scan each peak at a fixed scan rate of 2°/min. The scan width, w, for each peak was calculated from the expression $1.8 + 0.7 \tan \theta$. Ten-second background counts were measured at each end of a scan. The pulse-height analyzer of the scintillation detector was adjusted to accept 90% of the diffraction peak. The intensities of two standard reflections were measured after every 120 min of exposure time; their combined intensity decreased by 4% during the data collection period. The integrated intensity and standard deviation for each measured peak were calculated from the expressions $I = w(S/t_s - B/t_b)$ and $\sigma_c(I) = w(S/t_s^2 + B/t_b^2)^{1/2}$, respectively, where S represents the scan count accumulated in time t_s and B is the combined background count in time t_b. The intensity data were corrected for absorption, crystal decay, and Lorentz–polarization effects. The variances for F_o^2 were calculated from $\sigma^2(F_o^2) = \sigma_c^2(F_o^2) + (0.02F_o^2)^2$. Duplicate reflections were averaged to produce 3511 unique data of which 2301 reflections with $F_o^2 > 2\sigma(F_o^2)$ were included in the structural analysis.

Approximate positions for the two independent chromium atoms were determined from an analysis of an unsharpened Patterson map. The remaining nonhydrogen atoms were located by using conventional Fourier methods. All hydrogen atoms including the μ-H atom of the monoanion were subsequently located from a series of difference Fourier maps calculated with low-angle data (($\sin \theta$)/$\lambda < 0.40$ Å⁻¹). Full-matrix least-squares refinements[7-11] of the positional and anisotropic thermal parameters for the 49 nonhydrogen atoms and fixed contributions from the 37 hydrogen atoms led to final discrepancy indices[12] of $R(F_o) = 0.0405$, $R(F_o^2) = 0.0414$, $R_w(F_o^2) = 0.0569$, and $\sigma_1 = 1.25$ for 2301 reflections with $F_o^2 > 2\sigma(F_o^2)$. A final difference map confirmed the determined structure with no residuals being greater than 0.2 e/Å³. No correction for secondary extinction was required. The final X-ray determined positional and thermal parameters are

Table I. Crystal Data for $[K(crypt-222)]^+[Cr_2(CO)_{10}(\mu\text{-H})]^-$

cryst type	monoclinic
space group	$P2_1/c$ (C_{2h}^5, No. 14)
systematic abs	$\{h0l\}$, $l = 2n + 1$
	$\{0k0\}$, $k = 2n + 1$
fw	800.70
Z	4 molecules/unit cell
density (obsd), g/cm³	1.41
density (calcd), g/cm³	1.422

	X-ray	neutron
cryst dimens, mm	0.10 × 0.225 × 0.225	3.00 × 1.40 × 1.40
temp, K	293 ± 2	20 ± 1
a, Å	10.634 (3)	10.461 (4)
b, Å	14.595 (4)	14.416 (7)
c, Å	24.278 (7)	23.863 (7)
β, deg	97.00 (3)	97.24 (4)
V, Å³	3740 (2)	3570
μ, cm⁻¹	7.9	1.79
transmission coeff	0.85–0.92	0.695–0.766
radiatn	Mo Kα (Zr filtered)	neutron, Ge(220) crystal monochromator
wavelength, Å	0.710 69	1.1173 (2)
data collected	$\pm h, +k, +l$	$+h, +k, \pm l$
detector limits, deg	$3 \leq 2\theta \leq 40$	$2\theta \leq 103$
unique data	3511	4444
data used in anal.	2301 ($F_o^2 > 2\sigma(F_o^2)$)	4444

available as supplementary material and were used in the initial analysis of the neutron diffraction data.

Collection and Analysis of the Neutron Diffraction Data. A 9.0-mg crystal of $[K(crypt-222)]^+[Cr_2(CO)_{10}(\mu\text{-H})]^-$, with dimensions of 3.00 × 1.40 × 1.40 mm, was mounted on a hollow aluminum pin and was oriented approximately about the [100] crystallographic direction. The sample was placed in a specially constructed closed-cycle helium refrigerator[13] and mounted on an automated four-circle diffractometer[14] at the Brookhaven high-flux beam reactor. A Ge(220) crystal monochromator was employed to obtain a neutron beam of wavelength 1.1173 (2) Å (based upon KBr, $a = 6.600$ Å). The data were collected at a temperature of 20 ± 1 K.[15] The refined lattice dimensions (Table I) for the monoclinic unit cell were determined by a least-squares procedure based on $\sin \theta$ values of 32 reflections (30.0° ≤ 2θ ≤ 67.0°). Reflection intensities were measured in one quadrant of reciprocal space with $2\theta \leq 103°$, by employing a θ–2θ step scan technique. The 2θ scan range was 2.60° below 60° and 3.90° above 60°, with use of 65 steps of 0.04 (2θ) and 0.06° (2θ), respectively. Instrument and crystal stabilities were monitored by measuring two standard reflections every 80 measurements. A maximum fluctuation in their combined intensities of only 3% was observed. The integrated intensities for

(7) The least-squares refinements[8] of the X-ray diffraction data were based upon the minimization of $\sum w_i |F_o^2 - S^2 F_c^2|$ where the individual weights, w_i, equal $1/\sigma^2(F_o^2)$ and S is the scale factor.

(8) The scattering factors which were utilized in the calculations were those of Cromer and Mann[9] for the nonhydrogen atoms and those of Stewart et al.[10] for the hydrogen atoms with the corrections included for anomalous dispersion.[11]

(9) Cromer, D. T.; Mann, J. *Acta Crystallogr., Sect. A* **1968**, *A24*, 321.

(10) Stewart, R. F.; Davidson, E. R.; Simpson, W. T. *J. Chem. Phys.* **1965**, *42*, 3175.

(11) Cromer, D. T.; Liberman, D. *J. Chem. Phys.* **1970**, *53*, 1891.

(12) The discrepancy indices were calculated from the expressions $R(F_o) = [\sum ||F_o| - |F_c||/\sum |F_o|]$, $R(F_o^2) = \sum |F_o^2 - F_c^2|/\sum F_o^2$, $R_w(F_o) = [\sum w_i ||F_o| - |F_c||^2/\sum w_i |F_o|^2]^{1/2}$, and $R_w(F_o^2) = [\sum w_i |F_o^2 - F_c^2|^2/\sum w_i F_o^4]^{1/2}$. The final goodness-of-fit parameter, σ_1, equals $[\sum w_i |F_o^2 - F_c^2|/(n - p)]^{1/2}$ where n is the number of observations and p is the number of parameters varied.

(13) Air Products and Chemicals, Inc. DISPLEX Model CS-202.

(14) (a) Dimmler, D. G.; Grenlaw, N.; Kelley, M. A.; Potter, D. W.; Rankowitz, S.; Stubblefield, F. W. *IEEE Trans. Nucl. Sci.* **1976**, *NS23*, 398. (b) McMullan, R. K.; Andrews, L. C.; Koetzle, T. F.; Reidinger, F.; Thomas, R.; Williams, G. J. B. "NEXDAS, Neutron and X-ray Data Acquisition System", unpublished work.

(15) Calibration with reference to a magnetic phase transition in FeF₂ at T_N = 78.38 (1) K indicated that the recorded temperature is within 3 K of the actual value.

Table II. Positional Parameters ($\times 10^4$) and Thermal Parameters ($\text{Å}^2 \times 10^3$) from the Low-Temperature (20 K) Neutron Diffraction Study of [K(crypt-222)]$^+$[Cr$_2$(CO)$_{10}$(μ-H)]$^-$ ^{a}

ATOM	x	y	z	U_{11}	U_{22}	U_{33}	U_{12}	U_{13}	U_{23}
CR1	1637(3)	22(2)	2354(1)	6(1)	6(1)	3(1)	0(1)	1(1)	-2(1)
CR2	140(3)	1772(2)	1552(1)	7(1)	3(1)	3(1)	1(1)	3(1)	-1(1)
C1	2162(2)	885(1)	2950(1)	10(1)	7(1)	8(1)	-0(1)	-0(1)	0(1)
C2	98(2)	-267(1)	2575(1)	7(1)	10(1)	10(1)	1(1)	2(1)	0(1)
C3	1226(2)	-790(1)	1742(1)	10(1)	8(1)	8(1)	0(1)	1(1)	-1(1)
C4	3042(2)	367(1)	2002(1)	7(1)	9(1)	10(1)	-1(1)	2(1)	-0(1)
C5	2500(2)	-910(1)	2756(1)	8(1)	8(1)	10(1)	1(1)	1(1)	1(1)
C6	-1542(2)	1420(1)	1549(1)	7(1)	10(1)	9(1)	-1(1)	1(1)	-0(1)
C7	169(2)	1042(1)	442(1)	10(1)	7(1)	7(1)	0(1)	1(1)	-0(1)
C8	1482(2)	2210(1)	1501(1)	10(1)	10(1)	8(1)	-1(1)	1(1)	0(1)
C9	242(2)	2339(1)	2377(1)	14(1)	10(1)	8(1)	2(1)	1(1)	-1(1)
C10	-385(2)	2823(1)	1252(1)	11(1)	9(1)	9(1)	1(1)	-0(1)	2(1)
O1	2623(2)	1390(1)	3313(1)	15(1)	11(1)	10(1)	0(1)	-2(1)	-2(1)
O2	-436(2)	-433(1)	2458(1)	10(1)	17(1)	16(1)	-2(1)	5(1)	1(1)
O3	1046(2)	-1264(1)	1356(1)	15(1)	13(1)	10(1)	-2(1)	1(1)	-4(1)
O4	3453(2)	543(1)	1777(1)	10(1)	13(1)	14(1)	-1(1)	6(1)	1(1)
O5	3005(2)	-1503(1)	3057(1)	13(1)	10(1)	12(1)	3(1)	-2(1)	2(1)
O6	-2545(2)	1216(1)	1721(1)	11(1)	14(1)	15(1)	-1(1)	3(1)	-1(1)
O7	171(2)	590(1)	-546(1)	16(1)	13(1)	10(1)	0(1)	2(1)	-4(1)
O8	2459(2)	2537(1)	1553(1)	10(1)	14(1)	13(1)	-5(1)	0(1)	1(1)
O9	269(2)	2657(1)	2516(1)	23(1)	16(1)	10(1)	5(1)	-1(1)	-4(1)
O10	-722(2)	3478(1)	491(1)	17(1)	9(1)	13(1)	3(1)	-2(1)	4(1)
H	476(4)	729(3)	1497(2)	38(2)	39(2)	50(3)	4(2)	-2(2)	19(2)
K	4534(3)	1392(2)	4178(1)	5(1)	7(1)	8(1)	0(1)	2(1)	-1(1)
N1	2735(1)	3021(1)	4778(1)	8(1)	9(1)	9(1)	1(1)	1(1)	-1(1)
N2	5615(1)	946(1)	3520(1)	7(1)	8(1)	9(1)	0(1)	1(1)	0(1)
O11	2455(2)	919(1)	4731(1)	7(1)	7(1)	3(1)	-1(1)	1(1)	-1(1)
O12	4433(2)	24(1)	4025(1)	8(1)	3(1)	10(1)	0(1)	4(1)	0(1)
O13	3133(2)	3412(1)	3531(1)	9(1)	7(1)	10(1)	0(1)	2(1)	-0(1)
O14	5282(2)	2669(1)	3151(1)	9(1)	10(1)	9(1)	2(1)	1(1)	2(1)
O15	5509(2)	3269(1)	5077(1)	8(1)	12(1)	7(1)	0(1)	1(1)	-1(1)
O16	7273(2)	2050(1)	4550(1)	5(1)	9(1)	9(1)	-1(1)	-0(1)	-2(1)
C11	2085(2)	2328(1)	5116(1)	11(1)	9(1)	9(1)	2(1)	2(1)	-0(1)
C12	1729(2)	1434(1)	4749(1)	7(1)	10(1)	12(1)	-1(1)	1(1)	-0(1)
C13	2522(1)	57(1)	4405(1)	7(1)	8(1)	9(1)	-2(1)	2(1)	-1(1)
C14	3723(2)	-480(1)	4340(1)	8(1)	3(1)	10(1)	-1(1)	1(1)	-0(1)
C15	5490(2)	-500(1)	3557(1)	8(1)	8(1)	10(1)	2(1)	2(1)	1(1)
C16	6099(2)	38(1)	3426(1)	9(1)	10(1)	8(1)	1(1)	2(1)	0(1)
C17	1794(2)	3467(1)	4370(1)	9(1)	13(1)	11(1)	2(1)	0(1)	2(1)
C18	2409(2)	4017(1)	3434(1)	11(1)	10(1)	12(1)	3(1)	4(1)	2(1)
C19	3746(2)	3899(1)	3219(1)	11(1)	10(1)	14(1)	1(1)	6(1)	1(1)
C20	4243(2)	3198(1)	2941(1)	11(1)	13(1)	9(1)	3(1)	2(1)	3(1)
C21	5721(2)	1950(1)	2413(1)	11(1)	9(1)	8(1)	4(1)	1(1)	2(1)
C22	5907(2)	1497(1)	3131(1)	9(1)	11(1)	11(1)	3(1)	3(1)	3(1)
C23	3354(2)	3712(1)	5193(1)	8(1)	10(1)	14(1)	1(1)	-1(1)	-2(1)
C24	4553(2)	3403(1)	5459(1)	10(1)	14(1)	11(1)	1(1)	1(1)	-2(1)
C25	5605(2)	3175(1)	5332(1)	9(1)	12(1)	12(1)	0(1)	1(1)	-1(1)
C26	7645(2)	2329(1)	4545(1)	9(1)	9(1)	11(1)	-2(1)	1(1)	-3(1)
C27	6239(2)	1701(1)	4340(1)	8(1)	10(1)	11(1)	-1(1)	2(1)	-2(1)
C28	7775(2)	921(1)	4029(1)	8(1)	9(1)	10(1)	2(1)	-1(1)	1(1)
H1	1185(4)	2613(3)	5253(2)	23(2)	28(2)	28(2)	5(2)	10(2)	1(2)
H2	2724(4)	2151(3)	5499(1)	26(2)	25(2)	17(2)	3(2)	-2(1)	3(1)
H3	1160(4)	1562(3)	4343(2)	23(2)	24(2)	24(2)	0(2)	-5(1)	-2(2)
H4	1105(4)	1019(3)	5044(2)	22(2)	22(2)	31(2)	-2(2)	10(2)	4(2)
H5	194(3)	168(3)	4052(1)	21(2)	25(2)	18(2)	0(2)	-2(1)	-2(1)
H6	1930(4)	-359(3)	4725(1)	26(2)	20(2)	26(2)	-4(1)	11(2)	0(1)
H7	3441(4)	-1156(3)	4207(2)	28(2)	20(2)	33(2)	-3(2)	7(2)	-2(2)
H8	4314(4)	-592(3)	4492(1)	23(2)	28(2)	14(2)	2(2)	-1(1)	5(1)
H9	5125(3)	-1160(2)	3630(1)	22(2)	19(2)	26(2)	-0(1)	6(1)	-3(1)
H10	6156(3)	-657(3)	4243(1)	18(2)	27(2)	21(2)	4(1)	-1(1)	4(1)
H11	5360(3)	151(3)	3055(1)	21(2)	23(2)	19(2)	-1(1)	-2(1)	1(1)
H12	6855(4)	-403(3)	3276(1)	24(2)	22(2)	27(2)	4(2)	7(1)	-2(2)
H13	1204(3)	2926(3)	4139(1)	22(2)	25(2)	22(2)	-5(2)	-4(1)	-1(2)
H14	1143(4)	3931(3)	4555(2)	23(2)	30(2)	26(2)	10(2)	6(1)	3(2)
H15	1545(4)	4343(3)	3563(2)	26(2)	23(2)	25(2)	9(2)	4(2)	8(2)
H16	3031(4)	4573(3)	4124(2)	31(2)	23(2)	23(2)	-4(2)	6(2)	-4(2)
H17	4517(4)	4330(3)	3424(2)	31(2)	23(2)	35(2)	-5(2)	11(2)	-4(2)
H18	3047(4)	4330(3)	2957(2)	27(2)	28(2)	23(2)	12(2)	7(2)	10(2)
H19	3501(3)	2725(3)	2655(2)	20(2)	30(2)	24(2)	-0(2)	-4(1)	-2(2)
H20	4657(4)	3554(3)	2458(2)	36(2)	29(2)	24(2)	10(2)	10(2)	10(2)
H21	5465(4)	2241(3)	2415(1)	33(2)	27(2)	19(2)	5(2)	6(2)	3(2)
H22	4941(3)	1457(3)	2704(1)	22(2)	22(2)	25(2)	1(2)	-3(1)	-4(1)
H23	7356(4)	1057(3)	2433(1)	27(2)	26(2)	22(2)	10(2)	9(1)	5(1)
H24	7573(4)	2046(3)	3275(2)	25(2)	24(2)	25(2)	-4(2)	-0(1)	4(2)
H25	3534(4)	4343(3)	4955(2)	28(2)	19(2)	31(2)	-3(2)	0(2)	3(2)
H26	2738(4)	3917(3)	5518(2)	23(2)	29(2)	29(2)	1(2)	8(2)	-9(2)
H27	4585(4)	2760(3)	5729(2)	23(2)	27(2)	27(2)	-0(2)	5(1)	5(2)
H28	5037(4)	3936(3)	5743(2)	22(2)	35(2)	23(2)	-3(2)	1(1)	-12(2)
H29	7143(4)	3830(3)	5534(2)	21(2)	24(2)	27(2)	-3(2)	2(1)	-5(2)
H30	6378(3)	2436(3)	5561(1)	21(2)	27(2)	23(2)	2(2)	3(1)	8(2)
H31	7566(4)	3461(3)	4552(2)	30(2)	23(2)	26(2)	1(2)	8(2)	3(2)
H32	5652(4)	2908(3)	5057(2)	21(2)	27(2)	29(2)	-1(2)	0(1)	-8(2)
H33	8515(4)	2231(3)	4052(2)	30(2)	19(2)	26(2)	-5(2)	9(2)	-2(1)
H34	9099(3)	1532(3)	4534(2)	17(2)	33(2)	31(2)	1(2)	-4(2)	-7(2)
H35	9575(4)	536(3)	3326(2)	22(2)	29(2)	28(2)	5(2)	1(2)	-5(2)
H36	7553(4)	304(2)	4340(1)	28(2)	19(2)	21(2)	-2(1)	0(1)	6(1)

^{a} Thermal parameters correspond to the expression $T = -[2\pi^2(U_{11}h^2a^{*2} + \ldots + 2U_{12}hka^*b^* + \ldots)]$. Estimated standard deviations are in parentheses.

the 4739 measured reflections were corrected for Lorentz and absorption effects.[16] Duplicate and equivalent reflections were averaged to yield 4444 independent reflections.

The least-squares refinement was initiated by using the positional parameters obtained from the X-ray diffraction analysis, and isotropic thermal factors were initially set at $B = 1.25$ Å^3. The final cycle of block-diagonal least-squares refinement of 86 nine-by-nine blocks converged with discrepancy indices[12] of $R(F_o) = 0.039$ and $R_w(F_o)$

(16) A modification of an analytical method developed by: deMeulenaer, J.; Tompa, H. *Acta Crystallogr.* **1965**, *19*, 1014.

= 0.032 with σ_1 = 1.06.[17-19] During the analysis an isotropic extinction correction was included and refined to g = 0.43 × 10^{-4}.[20,21]

The final positional and thermal parameters derived from the low-temperature (20 K) neutron diffraction analysis are listed in Table II. Internuclear distances and bond angles with esd's calculated from the errors for the fractional atomic coordinates are compared for the nonhydrogen atoms in Table III. The corresponding parameters for the hydrogen atoms and the structure factor tables for both data sets are available as supplementary material. Least-squares planes of interest, calculated from the neutron-determined coordinates for the anion, are provided in Table IV.[22,23]

Discussion of Results

General Description of the Crystal Structure. The crystal structure of [K(crypt-222)]$^+$[Cr$_2$(CO)$_{10}$(μ-H)]$^-$, as determined from the low-temperature (20 K) neutron diffraction data, is shown stereographically in Figure 1. From this unit cell diagram, which shows the arrangement of four [K(crypt-222)]$^+$ cations and four [Cr$_2$(CO)$_{10}$(μ-H)]$^-$ anions in the centrosymmetric monoclinic unit cell, it is quite evident that one of the carbonyl groups is directed toward the K$^+$ ion in the cation. Although the corresponding K···O1–C1 angle of 148.9 (2) Å is not linear, the relatively close K···O1 separation of 2.966 (3) Å is nearly equal to the sum of their ionic radii (ca. 2.9 Å). In fact, since this separation is less than 0.1 Å longer than the corresponding K–O bond distances which range from 2.794 (4) to 2.886 (3) Å within the cation, one might conclude that O1 is *weakly* coordinated to the K$^+$ ion. The shortest remaining contacts between the carbonyl oxygen atoms and the hydrogen atom perimeter of the cation (viz., O3···H33, 2.445 (5) Å; O4···H17, 2.459 (5) Å; O5···H21, 2.454 (4) Å) are probably a consequence of the K$^+$···O1 interaction and thereby do not suggest the presence of any other unusual interactions.

The extent of this attractive interaction is indicated by the conformational changes associated with the anion and the cation. Since the K$^+$ ion interacts with only one Cr(CO)$_5$ fragment of the anion, it has an unsymmetrical influence on the anion's overall geometry. In solution, the IR data for the [K(crypt-222)]$^+$ salt is consistent with an eclipsed metal carbonyl configuration.[24] However, as the crystal lattice is formed, the Cr(CO)$_5$ unit that contains O1 is attracted toward the K$^+$ ion at the center of the cryptate's cavity. As a result of the K$^+$ ion's influence, the eclipsed carbonyl configuration undergoes a twisting distortion to the observed bent structure. Since the bond distances and bond angles within the two independent Cr(CO)$_5$ moieties are comparable in magnitude, they collectively indicate that the attractive interaction between
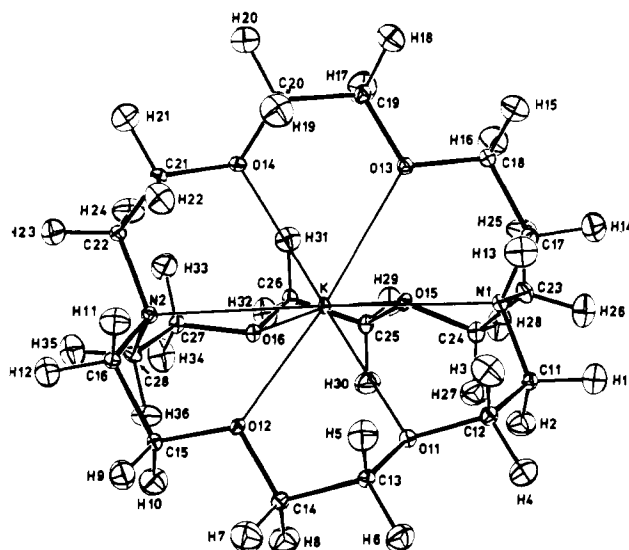

Figure 2. Molecular configuration of the [K(crypt-222)]$^+$ cation with the atom labeling scheme.

O1 and K$^+$ is insufficient to perturb appreciably the local C_{4v} symmetry of the corresponding Cr(CO)$_5$ unit. Thus, this unexpected distortion of the anion's crystal structure provides further evidence of the flexible nature of the Cr–H–Cr bond.

Although the X-ray and neutron diffraction measurements were carried out at widely different temperatures, the corresponding structural parameters associated with the nonhydrogen atoms in Table III agree within experimental error for the most part. The relative constancy of their values (particularly the bond angles) between 20–293 K indicates that the anion's solid-state structure is not perturbed significantly by reduction of the temperature of the crystal lattice. However, lowering the sample temperature has damped out an appreciable amount of the nuclear thermal motion and thus has allowed us to determine the nuclear positions with a higher overall degree of precision. Consequently the esd's of the neutron-determined parameters for the nonhydrogen atoms are generally smaller than the corresponding X-ray determined parameters by a factor of at least 2.

Conformational Structure of the [K(crypt-222)]$^+$ Cation. Our structural analysis provides an opportunity to examine the effect of the K$^+$···O1 interaction upon the conformational structure of the [K(crypt-222)]$^+$ cation. A perspective view of the cation with the appropriate atom labeling scheme is depicted in Figure 2. In accord with an X-ray diffraction study of the [K(crypt-222)]I[25] the K$^+$ is embedded within the cryptate molecule and is coordinated to six O atom and two N atom donors. The typical "in-in" nitrogen configuration is preserved with N1 and N2 displaced 0.477 (2) and 0.476 (2) Å from the C11, C17, C23 and C16, C22, C28 planes, respectively, toward the K$^+$ ion. The N1–K–N2 bond angle is 177.0 (1)°. However, a comparison of the corresponding K–O and K–N bond distances with those determined for the iodide salt[25] clearly suggests that the presence of O1 in the K$^+$ coordination sphere leads to a noticeable elongation of the cryptate ion. This structural adjustment increases the N···N separation by ca. 0.27 Å and the two independent K–N distances of 3.002 (3) and 3.018 (3) Å by ca. 0.15 Å compared to their corresponding values in the iodide salt.[25] The lengthening of the N···N separation is accompanied by a noticeable decrease in the six C–C–N bond angles and an increase in the six N–C–C–O and three O–C–C–O torsional angles (Table V). Another consequence of the cation–anion

(17) The neutron scattering amplitudes used[18] in this study were $\bar{b}_{Cr}$ = 0.352, $\bar{b}_K$ = 0.370, $\bar{b}_O$ = 0.575, $\bar{b}_N$ = 0.940, $\bar{b}_C$ = 0.663, and $\bar{b}_H$ = –0.372 (all units in 10^{-12} cm).

(18) Bacon, G. E. *Acta Crystallogr., Sect. A* **1972**, *A28*, 357.

(19) The least-squares refinements of the neutron diffraction data were based upon the minimization of $\sum w_i ||F_o| - |F_c||$, where the individual weights w_i = $1/\sigma^2(|F_o|)$.

(20) The Zachariasen approximation[21a] was used for the overall isotropic g parameter as defined by Coppens and Hamilton.[21b] The F_o values were corrected for extinction from the expression $|F_o|_{cor}$ = $|F_o|(1 + T2g\lambda^3|F_c|^2/V^2 \sin 2\theta)^{-1/4}$, where F_c is on an absolute scale, λ is the wavelength (Å), g is the refined extinction parameter, $\bar{T}$ is the mean absorption-weighted path length in the crystal in centimeters, and V is the unit cell volume (Å^3).

(21) (a) Zachariasen, W. H. *Acta Crystallogr.* **1967**, *23*, 558. (b) Coppens, P.; Hamilton, W. C. *Acta Crystallogr., Sect. A* **1970**, *A26*, 71.

(22) For the determination of the "best" equation for each least-squares plane, the perpendicular distances of atoms from the plane, and the acute dihedral angles between the planes, the program PLNJO was employed. The program was written by J. O. Lundgren, University of Uppsala, Uppsala, Sweden, and is based on the method of Blow.[23]

(23) Blow, D. *Acta Crystallogr.* **1960**, *16*, 168.

(24) In solution the IR spectrum of the Na$^+$, [Et$_4$N]$^+$, and [(Ph$_3$P)$_2$N]$^+$ salts exhibit only three carbonyl stretching vibrational bands (cm^{-1}). Na$^+$: 2032 (w), 1942 (vs), 1879 (s). [Et$_4$N]$^+$: 2033 (w), 1943 (vs), 1881 (s). [(Ph$_3$P)$_2$N]$^+$: 2033 (w), 1942 (vs), 1875 (s).[6]

(25) Moras, P. D.; Metz, B.; Weiss, R. *Acta Crystallogr., Sect. B* **1973**, *B29*, 383.

Table III. Interatomic Distances (A) and Bond Angles (Deg) for [K(crypt-222)]⁺[Cr₂(CO)₁₀(μ-H)]⁻ ᵃ

(A) Distances for the [Cr₂(CO)₁₀(μ-H)]⁻ Monoanion

	neutron	X-ray		neutron	X-ray
Cr1-H	1.735 (5)	1.77	Cr2-H	1.723 (5)	1.60
Cr1-C1	1.900 (3)	1.887 (6)	Cr2-C6	1.899 (3)	1.895 (7)
Cr1-C2	1.903 (4)	1.876 (6)	Cr2-C7	1.895 (3)	1.866 (6)
Cr1-C3	1.897 (3)	1.877 (6)	Cr2-C8	1.898 (3)	1.882 (7)
Cr1-C4	1.899 (4)	1.880 (7)	Cr2-C9	1.907 (3)	1.889 (7)
Cr1-C5	1.846 (3)	1.845 (6)	Cr2-C10	1.851 (3)	1.826 (7)
C1-O1	1.148 (2)	1.129 (8)	C6-O6	1.147 (3)	1.136 (9)
C2-O2	1.145 (3)	1.130 (9)	C7-O7	1.145 (3)	1.145 (8)
C3-O3	1.143 (3)	1.141 (8)	C8-O8	1.145 (3)	1.141 (9)
C4-O4	1.143 (3)	1.146 (9)	C9-O9	1.142 (3)	1.136 (9)
C5-O5	1.159 (3)	1.145 (8)	C10-O10	1.161 (3)	1.147 (8)
Cr1⋯Cr2	3.300 (4)	3.314 (1)			

(B) Distances for the [K(crypt-222)]⁺ Cation

	neutron	X-ray		neutron	X-ray		neutron	X-ray
K-N1	3.018 (3)	3.000 (6)	K-N2	3.002 (3)	2.979 (5)			
K-O11	2.869 (4)	2.862 (4)	K-O13	2.803 (3)	2.781 (4)	K-O15	2.886 (3)	2.875 (4)
K-O12	2.866 (4)	2.821 (4)	K-O14	2.796 (4)	2.788 (4)	K-O16	2.843 (3)	2.845 (4)
N1-C11	1.471 (2)	1.481 (9)	N1-C17	1.475 (2)	1.472 (8)	N1-C23	1.469 (2)	1.465 (9)
N2-C16	1.469 (2)	1.475 (9)	N2-C22	1.475 (2)	1.465 (9)	N2-C28	1.470 (2)	1.468 (8)
C11-C12	1.516 (2)	1.485 (10)	C13-C14	1.505 (2)	1.490 (9)	C15-C16	1.517 (2)	1.500 (9)
C17-C18	1.515 (3)	1.493 (11)	C19-C20	1.509 (3)	1.476 (11)	C21-C22	1.518 (2)	1.485 (10)
C23-C24	1.514 (2)	1.485 (10)	C25-C26	1.507 (3)	1.464 (11)	C27-C28	1.517 (3)	1.497 (10)
O11-C12	1.421 (3)	1.416 (8)	O13-C18	1.413 (3)	1.407 (9)	O15-C24	1.419 (3)	1.409 (9)
O11-C13	1.419 (3)	1.422 (8)	O13-C19	1.418 (3)	1.420 (9)	O15-C25	1.422 (3)	1.396 (9)
O12-C14	1.415 (3)	1.412 (8)	O14-C20	1.416 (2)	1.418 (8)	O16-C26	1.422 (3)	1.416 (9)
O12-C15	1.420 (3)	1.413 (8)	O14-C21	1.424 (3)	1.419 (8)	O16-C27	1.419 (3)	1.403 (8)

(C) Bond Angles for the [Cr₂(CO)₁₀(μ-H)]⁻ Monoanion

	neutron	X-ray		neutron	X-ray
Cr1-H-Cr2	145.2 (3)	158.5			
H-Cr1-C1	96.1 (2)	92.9	H-Cr2-C6	81.3 (2)	85.8
H-Cr1-C2	75.6 (2)	81.1	H-Cr2-C7	84.0 (2)	85.1
H-Cr1-C3	83.8 (2)	86.4	H-Cr2-C8	102.4 (2)	96.8
H-Cr1-C4	99.4 (2)	94.3	H-Cr2-C9	87.6 (2)	86.8
H-Cr1-C5	164.9 (2)	171.8	H-Cr2-C10	170.8 (2)	175.3
C1-Cr1-C2	92.1 (1)	90.7 (3)	C6-Cr2-C7	90.0 (1)	89.4 (3)
C1-Cr1-C3	174.8 (2)	177.2 (3)	C6-Cr2-C8	176.1 (2)	177.0 (3)
C1-Cr1-C4	89.5 (1)	90.3 (3)	C6-Cr2-C9	88.9 (1)	88.2 (3)
C1-Cr1-C5	89.9 (1)	90.1 (3)	C6-Cr2-C10	89.9 (1)	90.4 (3)
C2-Cr1-C3	92.9 (1)	91.9 (3)	C7-Cr2-C8	92.0 (2)	92.9 (3)
C2-Cr1-C4	175.0 (2)	175.3 (3)	C7-Cr2-C9	171.6 (2)	171.6 (3)
C2-Cr1-C5	90.4 (1)	91.2 (3)	C7-Cr2-C10	93.3 (1)	93.1 (3)
C3-Cr1-C4	85.4 (1)	87.0 (3)	C8-Cr2-C9	89.7 (1)	89.7 (3)
C3-Cr1-C5	91.4 (1)	90.9 (3)	C8-Cr2-C10	86.5 (1)	87.5 (3)
C4-Cr1-C5	94.4 (1)	93.3 (3)	C9-Cr2-C10	95.0 (1)	95.0 (3)
Cr1-C1-O1	176.9 (2)	176.9 (6)	Cr2-C6-O6	179.0 (2)	178.9 (6)
Cr1-C2-O2	179.2 (2)	179.6 (6)	Cr2-C7-O7	178.7 (2)	178.3 (6)
Cr1-C3-O3	176.0 (2)	177.1 (6)	Cr2-C8-O8	174.6 (2)	174.5 (6)
Cr1-C4-O4	177.6 (2)	177.9 (6)	Cr2-C9-O9	178.3 (2)	177.4 (6)
Cr1-C5-O5	177.9 (2)	178.1 (6)	Cr2-C10-O10	178.3 (2)	177.8 (6)

(D) Bond Angles for the [K(crypt-222)]⁺ Cation

	neutron	X-ray		neutron	X-ray		neutron	X-ray
N1-K-N2	177.0 (1)	176.9 (1)						
N1-K-O11	62.1 (1)	61.3 (1)	N1-K-O13	60.2 (1)	60.7 (1)	N1-K-O15	59.2 (1)	59.3 (1)
N2-K-O12	59.4 (1)	59.8 (1)	N2-K-O14	62.1 (1)	61.6 (1)	N2-K-O16	60.2 (1)	60.3 (1)
N1-K-O12	120.4 (1)	119.8 (1)	N1-K-O14	120.3 (1)	120.9 (1)	N1-K-O16	117.2 (1)	117.2 (1)
N2-K-O11	117.2 (1)	117.9 (1)	N2-K-O13	122.6 (1)	122.1 (1)	N2-K-O15	118.7 (1)	118.6 (1)
O11-K-O12	58.8 (1)	58.9 (1)	O12-K-O13	129.4 (1)	130.7 (1)	O13-K-O15	89.3 (1)	88.9 (1)
O11-K-O13	104.4 (1)	104.8 (1)	O12-K-O14	104.9 (1)	105.2 (1)	O13-K-O16	128.5 (1)	127.3 (1)
O11-K-O14	146.6 (1)	146.5 (1)	O12-K-O15	137.5 (1)	136.7 (1)	O14-K-O15	110.0 (1)	110.3 (1)
O11-K-O15	99.4 (1)	99.0 (1)	O12-K-O16	97.7 (1)	97.7 (1)	O14-K-O16	90.5 (1)	90.2 (1)
O11-K-O16	119.2 (1)	119.6 (1)	O13-K-O14	61.3 (1)	61.2 (1)	O15-K-O16	59.2 (1)	59.0 (1)
C11-N1-C17	110.0 (1)	111.0 (5)	C11-N1-C23	109.2 (1)	110.1 (5)	C17-N1-C23	110.8 (1)	110.2 (5)
C16-N2-C22	109.5 (1)	109.5 (5)	C16-N2-C28	110.0 (1)	109.6 (5)	C22-N2-C28	110.8 (1)	110.8 (5)
N1-C11-C12	114.9 (1)	114.4 (5)	N1-C17-C18	113.6 (1)	115.7 (5)	N1-C23-C24	113.7 (1)	114.2 (6)
C11-C12-O11	110.3 (1)	109.6 (5)	C17-C18-O13	109.3 (1)	108.8 (5)	C23-C24-O15	108.6 (1)	108.7 (5)
C12-O11-C13	110.4 (2)	110.2 (5)	C18-O13-C19	112.0 (2)	112.7 (5)	C24-O15-C25	111.4 (2)	112.3 (5)
O11-C13-C14	109.9 (1)	109.4 (5)	O13-C19-C20	108.9 (1)	109.2 (5)	O15-C25-C26	109.4 (1)	113.5 (5)
C13-C14-O12	108.7 (1)	108.7 (5)	C19-C20-O14	110.2 (1)	110.4 (5)	C25-C26-O16	109.4 (1)	110.4 (6)
C14-O12-C15	111.9 (2)	111.7 (4)	C20-O14-C21	111.0 (1)	112.0 (5)	C26-O16-C27	110.1 (2)	112.0 (5)
O12-C15-C16	108.8 (1)	109.3 (5)	O14-C21-C22	109.0 (3)	109.8 (5)	O16-C27-C28	110.4 (1)	111.3 (5)
C15-C16-N2	114.1 (1)	113.5 (5)	C21-C22-N2	113.0 (1)	114.2 (5)	C27-C28-N2	114.1 (1)	113.3 (5)

ᵃ The corresponding bonding parameters for the hydrogen atoms in the [K(crypt-222)]⁺ cation are provided in the supplementary material.

Table IV. Least-Squares Molecular Planes for
[K(crypt-222)]$\bullet$[Cr$_2$(CO)$_{10}$(μ-H)]$^{-\ a}$

I. Equations of Least-Squares Planes and Perpendicular
Distances (Å) of Atoms of the Planes Calculated
for the [Cr$_2$(CO)$_{10}$(μ-H)]$^-$ Anion

1. Plane through Cr1, C1, C2, C3, and C4
$-4.6874x + 10.1010y - 10.9215z + 3.2811 = 0$

Cr1	−0.044 (3)	H	1.642 (5)
C1	−0.025 (2)	O1	−0.071 (2)
C2	0.034 (2)	O2	0.098 (2)
C3	−0.026 (2)	O3	−0.018 (2)
C4	0.037 (2)	O4	0.059 (2)
C5	−1.889 (2)	O5	−3.045 (2)

2. Plane through Cr2, C6, C7, C8, and C9
$3.0360x − 11.7776y + 10.9236z + 0.1884 = 0$

Cr2	−0.036 (3)	H	1.657 (5)
C6	−0.097 (2)	O6	−0.152 (2)
C7	0.101 (2)	O7	0.196 (2)
C8	−0.094 (2)	O8	−0.236 (2)
C9	0.104 (2)	O9	0.218 (2)
C10	−1.886 (2)	O10	−3.045 (2)

3. Plane through Cr1, C2, C4, and C5
$-1.7842x − 9.4940y − 16.8377z + 4.2742 = 0$

Cr1	−0.020 (3)	H	0.136 (5)
C1	−1.919 (3)	O1	−3.063 (3)
C2	0.006 (3)	O2	0.023 (3)
C3	1.873 (3)	O3	3.005 (3)
C4	0.006 (3)	O4	0.062 (3)
C5	0.001 (3)	O5	0.017 (3)

4. Plane through Cr1, C1, C3, and C5
$9.5008x + 2.9164y − 11.4043z + 1.0676 = 0$

Cr1	−0.066 (4)	H	−0.547 (5)
C1	0.016 (3)	O1	0.090 (3)
C2	−1.968 (3)	O2	−3.113 (3)
C3	0.016 (3)	O3	0.146 (3)
C4	1.820 (3)	O4	2.956 (3)
C5	0.001 (3)	O5	−0.001 (3)

5. Plane through Cr2, C6, C8, and C10
$1.1235x − 7.3930y − 20.4861z + 4.6948 = 0$

Cr2	0.022 (3)	H	0.119 (5)
C6	−0.009 (3)	O6	−0.021 (3)
C7	1.914 (3)	O7	3.057 (3)
C8	−0.009 (3)	O8	−0.041 (3)
C9	−1.876 (3)	O9	−3.009 (3)
C10	0.001 (3)	O10	0.013 (3)

6. Plane through Cr2, C7, C9, and C10
$10.0712x + 3.8416y − 3.9844z − 0.1982 = 0$

Cr2	0.016 (4)	H	−0.236 (5)
C6	−1.883 (3)	O6	−3.030 (3)
C7	−0.004 (3)	O7	−0.037 (3)
C8	1.909 (3)	O8	3.038 (3)
C9	−0.004 (3)	O9	−0.029 (3)
C10	−0.001 (3)	O10	0.016 (3)

7. Plane through Cr1, Cr2, and H
$2.9201x − 6.1950y − 21.1679z + 4.5397 = 0$

Cr1	−0.001 (3)	Cr2	−0.001 (3)
C1	−1.622 (3)	C6	−0.386 (3)
C2	−0.930 (3)	C7	1.850 (3)
C3	1.701 (3)	C8	0.331 (3)
C4	0.976 (3)	C9	−1.870 (3)
C5	−0.0655 (3)	C10	0.029 (3)
H	−0.001 (5)		

II. Acute Dihedral Angles (Deg) between Planes

1 and 2	10.4	2 and 4	85.2	3 and 7	30.1
1 and 3	88.7	2 and 5	88.5	4 and 5	72.2
1 and 4	86.0	2 and 6	87.8	4 and 6	19.1
1 and 5	88.9	2 and 7	89.8	4 and 7	61.2
1 and 6	77.7	3 and 4	88.9	5 and 6	89.7
1 and 7	89.6	3 and 5	19.3	5 and 7	11.0
2 and 3	82.9	3 and 6	72.2	6 and 7	78.8

^{a} The equations of the planes are expressed in monoclinic fractional coordinates x, y, z. ^{b} The standard deviations are weighted according to the estimated errors associated with the fractional coordinates.
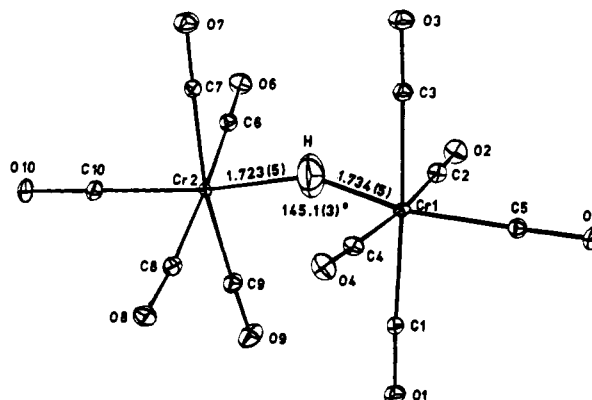

Figure 3. Perspective view of the [Cr$_2$(CO)$_{10}$(μ-H)]$^-$ anion with the atom labeling scheme. The μ-H atom is symmetrically located in a bent Cr–H–Cr bond.

interaction is the larger range of 0.09 Å observed for the six K–O bond distances within the cation for [K(crypt-222)]$^+$-[Cr$_2$(CO)$_{10}$(μ-H)]$^-$ compared to that of 0.014 Å for the three independent K–O bond distances (2.785 Å (average)) for [K(crypt-222)]I.[25] This 0.09-Å variation of the K–O distances is consistent with an asymmetrical coordination environment about the K$^+$ ion arising from the close proximity of O1. Finally, the geometry of the six oxygen atoms of the cation conforms closely to a trigonal prism. The smaller twist angle of 10.8° (average)[26] and larger separation between the O$_3$ faces of the prism of 2.795 (3)° (compared to 22.5° and 2.65 Å, respectively, in the iodide salt[25]) are further indications of the cation's elongation. Despite these conformational adjustments, the individual N–C, C–C, and C–O bond distances and C–N–C, N–C–C, C–C–O, and C–O–C bond angles within the cryptate molecule do not significantly deviate from their averaged values.[27] To a certain extent the conformational behavior of the cryptate molecule resembles an accordion, with the degree of elongation or compression depending upon the ionic radius of the central metal ion and its coordination environment.

Molecular Configuration of the [Cr$_2$(CO)$_{10}$(μ-H)]$^-$ Anion. A perspective view of the [Cr$_2$(CO)$_{10}$(μ-H)]$^-$ anion with the appropriate atom labeling scheme is shown in Figure 3. Despite the fact that the K$^+$ ion is enveloped by the cryptate's cage, we have seen that the K$^+$ ion plays an influential role in dictating the anion's solid-state configuration. Under these circumstances, the anion has adopted a bent metal carbonyl configuration which is intermediate between the linear, eclipsed configuration in [(Ph$_3$P)$_2$N]$^+$[Cr$_2$(CO)$_{10}$(μ-H)]$^{-3b,c}$ and the bent, staggered configuration in [(Ph$_3$P)$_2$N]$^+$[W$_2$(CO)$_{10}$(μ-H)]$^{-5b}$. The bridging hydrogen atom resides in a symmetrical electronic environment as supported by the Cr–H separations of 1.735 (5) and 1.723 (5) Å which are equivalent within experimental error and are comparable in magnitude to the corresponding distances in the [Et$_4$N]$^+$ and [(Ph$_3$P)$_2$N]$^+$ salts.[3] The greater π-acceptor ability of the CO ligand trans to the bridging hydrogen atom is supported by the significantly shorter average Cr–C$_{ax}$ distance of 1.848 (3) Å and longer C$_{ax}$–O$_{ax}$ distance of 1.160 (3) Å compared to the averaged

(26) The twist angle refers to the average torsional angle between two O–CNT vectors, where CNT is the centroid of the respective triangular face of the prism and O refers to one of the pair of oxygen atoms which share an edge of the prism.

(27) The average C–N, C–C, and C–O bond distances are 1.472 (1), 1.513 (2), and 1.419 (1) Å, respectively. The average C–N–C, N–C–C, C–C–O, and C–O–C bond angles in the [K(crypt-222)]$^+$ cation are 110.1 (4), 113.9 (3), 109.4 (2), and 111.1 (3)°, respectively. The standard deviation of the average, σ_l, was calculated from the expression $\sigma_l = [\sum (l - l_m)^2/(m^2 - m)]^{1/2}$, where m is the number of equivalent bonds (or angles), l_m is the value of the mth bond (or angle), and l is the corresponding mean value.

Table V. Torsional Angles (Deg) within the [K(crypt-222)]$^+$ Cation^a

N1-C11-C12-O1	69.9 (2)	C11-C12-O11-C13	176.5 (2)
O11-C13-C14-O12	-63.2 (2)	C13-C14-O12-C15	-171.3 (2)
O12-C15-C16-N2	60.6 (2)	C17-C18-O13-C19	-179.3 (2)
N1-C17-C18-O13	62.5 (2)	C19-C20-O14-C21	174.9 (2)
O13-C19-C20-O14	-65.9 (2)	C23-C24-O15-C25	167.3 (1)
O14-C21-C22-N2	69.8 (2)	C25-C26-O16-C27	-165.2 (2)
N1-C23-C24-O15	62.8 (2)	C12-O11-C13-C14	179.6 (2)
O15-C25-C26-O16	-63.6 (2)	C14-O12-C15-C16	173.6 (2)
O16-C27-C28-N2	60.4 (2)	C18-O13-C19-C20	-169.2 (2)
C11-N1···N2-C16	37.0 (2)	C20-O14-C21-C22	172.2 (2)
C17-N1···N2-C22	38.5 (1)	C24-O15-C25-C26	173.9 (1)
C23-N1···N2-C28	36.1 (2)	C26-O16-C27-C28	-173.2 (2)
O11···CNT1···CNT2···O12	10.0 (2)	O15···CNT1···CNT2···O16	11.6 (2)
O13···CNT1···CNT2···O14	10.8 (2)		

^{a} CNT1 and CNT2 represent the centroid of the triangles containing O11, O13, O15 and O12, O14, O16, respectively.

equatorial distances of 1.900 (3) and 1.145 (2) Å, respectively. However, the close agreement between the appropriate bond distances within the two independent Cr(CO)$_5$ fragments indicates that the cation-anion interaction has had no observable effect upon the bonding within either metal carbonyl fragment. Although this interaction may be important so far as crystal packing effects are concerned, it does not appear to alter appreciably the electronic structure of the anion.

This intermediate geometry for the [Cr$_2$(CO)$_{10}$(μ-H)]$^-$ represents a previously unobserved one for a [M$_2$(CO)$_{10}$(μ-H)]$^-$ anion and therefore is characterized by a distinctly different carbonyl ligand disposition, M-H-M bond angle, and metal-metal separation. In contrast to the eclipsed carbonyl structure observed for the [Cr$_2$(CO)$_{10}$(μ-H)]$^-$ anion in the [Et$_4$N]$^+$ and [(Ph$_3$P)$_2$N]$^+$ salts,[3] the two independent Cr(CO)$_5$ groups of the anion in the [K(crypt-222)]$^+$ salt are rotated ca. 19° about the Cr-Cr axis with respect to one another. This variation is accompanied by a reduction (0.05-0.09 Å) of the Cr···Cr separation to 3.300 (4) Å with a Cr-H-Cr bond angle of 145.2 (3)°, which is midway between the Cr-H-Cr bond angle of 158.9 (6)° in the [Et$_4$N]$^+$ salt[3a] and the W-H-W bond angle of 123.4 (5)° in the [Ph$_4$P]$^+$ salt.[3b] These decreases are consistent with the structural data reported by Bau and co-workers[5] for various salts of the [W$_2$(CO)$_{10}$(μ-H)]$^-$ anion. Their structural studies have shown that as the [W$_2$(CO)$_{10}$-(μ-H)]$^-$ anion's geometry is transformed from a linear, eclipsed to a bent, staggered metal carbonyl configuration, the W···W separation decreases by ca. 0.11 Å with a substantial reduction of the W-H-W bond angle. The reduction in the M···M separation that accompanies the decrease of the M-H-M bond angle in these anions implies a concomitant increase of the metal-metal bonding component.

A comparison of the X-ray and neutron determined Cr-H-Cr bond angles indicates that the maximum overlap region in the three-center, two-electron Cr-H-Cr bond is displaced toward the centroid of the Cr-H-Cr triangle. Consequently, for "closed" M-H-M bonds,[28] X-ray diffraction methods give shorter average M-H distances and larger M-H-M bond angles than neutron diffraction.[29] The octahedral-like coordination about each of the Cr atoms in the anion provides a suitable internal coordinate system which may be used to estimate the location of the electron density maximum in the Cr-H-Cr bond. The intersection of the two projected Cr-C$_{ax}$ vectors, which intersect at an angle of 169.3 (2)°, is displaced

only ca. 0.2 Å from the Cr-Cr line, whereas the nucleus of the bridging H atom is displaced 0.52 Å from the Cr-Cr line. Thus, these structural data are consistent with the "closed" representation of the bent Cr-H-Cr bond with the maximum overlap region displaced toward the centroid of Cr-H-Cr triangle.

In agreement with our previous neutron diffraction studies of the [Et$_4$N]$^+$ and [(Ph$_3$P)$_2$N]$^+$ salts,[3] the bridging H atom position is staggered with respect to the Cr-CO$_{eq}$ directions (as indicated by the nonzero dihedral angles in Table IV between the Cr1-H-Cr2 plane and the corresponding planes containing the equatorial carbonyl groups). As the symmetry of the metal carbonyl framework is reduced from D_{4h} (eclipsed) to C_{2v} (bent), the number of staggered positions available to the μ-H atom is reduced from four equivalent sites ([(Ph$_3$P)$_2$N]$^+$ salt) to one sterically preferred site ([Et$_4$N]$^+$ and [K(crypt-222)]$^+$ salts).

The ordered structure for the μ-H atom which results has provided a unique opportunity to obtain detailed information regarding its thermal motion at low temperature. Consistent with other neutron diffraction studies of M-H-M bonds,[3,5] its maximum root-mean-square thermal displacement, $u(3)$, is directed normal to the M-H-M plane (viz., 89 (2)°) in the [K(crypt-222)]$^+$ salt. The μ-H atom's thermal displacements are noticeably larger than those for the remaining atoms and probably reflect the effects of its greater zero-point energy. This result is reasonable considering the fact that the μ-H atom is the sole bridging link between two much heavier Cr(CO)$_5$ moieties. In contrast, for transition-metal hydrides with bent M-H-M bonds that are bridged by additional ligands such as the dimethylphosphido bridge in Mo$_2$(η^5-C$_5$H$_5$)$_2$(CO)$_4$(μ-H)(μ-PMe$_2$),[30] the relative size of the thermal ellipsoid for the μ-H atom is reduced appreciably since under these circumstances the M-H-M bond appears to be more rigid. Since substitution of deuterium for hydrogen in the anion should reduce the thermal motion of the bridging atom, one might expect to observe an isotope effect for the anion. Consequently, the corresponding fully deuterated analogue is being prepared for future structural studies to determine the extent of this effect, if any, upon the metal carbonyl structure and the Cr-H-Cr bond.

In summary, our structural analysis of [K(crypt-222)]$^+$-[Cr$_2$(CO)$_{10}$(μ-H)]$^-$ has demonstrated that cation-anion interactions may have a significant influence upon the anion's solid-state geometry. The preferred configuration of the anion in the absence of crystallographic site symmetry in this case represents an intermediate one, defined by the ability of the K$^+$···O1 interaction to overcome the low-energy barrier required to perturb the metal carbonyl framework. The rela-

(28) This type of three-center, two-electron bond is represented formally by

which indicates the presence of a significant metal-metal bonding component.

(29) Petersen, J. L.; Williams, J. M. *Inorg. Chem.* **1978**, *17*, 1308.

(30) Petersen, J. L.; Dahl, L. F.; Williams, J. M. *J. Am. Chem. Soc.* **1974**, *96*, 6610.

tively large thermal displacements for the μ-H atom are consistent with the deformability of the Cr–H–Cr linkage. Despite the fact that it is surrounded by the cryptate molecule, the K⁺ ion is not totally screened from interacting with atoms outside its immediate coordination environment. Consequently, whenever a cryptate cation is employed as the counterion for structural studies of polynuclear anions, the potential importance of cation–anion interactions should not be overlooked.

Contribution from the Istituto di Chimica Generale, Università di Pisa, 56100 Pisa, Italy, and the Istituto di Strutturistica Chimica, Università di Parma, 43100 Parma, Italy

Activation of CO₂-like Molecules: Synthetic and Structural Studies on a η^2-C,N Metal-Bonded Carbodiimide and Its Conversion into a η^2-C,N Metal-Bonded Amidinyl Ligand

MARCO PASQUALI, SANDRO GAMBAROTTA, CARLO FLORIANI,* ANGIOLA CHIESI-VILLA, and CARLO GUASTINI

Vanadocene reacts with *p*-tolylcarbodiimide (*p*-TCD) producing a metallaazacyclopropane-like complex Cp₂V(RN—C=NR) (I) (R = *p*-CH₃C₆H₄; Cp = η^5-C₅H₅; ν_{CN}(Nujol) 1645 cm⁻¹; μ_{eff} = 1.76 μ_B at 293.5 K). The X-ray analysis performed on complex I shows that vanadium is η^5 bonded to the two Cp rings, which are in a bent arrangement, making a cavity in the equatorial plane for the CN₂ unit. The C—N bond distances agree with the presence of a single C—N bond interacting with the metal and a free C=N double bond. Complex I reacts with both O₂ and I₂, releasing *p*-TCD. Coordinated *p*-TCD is converted in a η^2-C,N metal-bonded trialkylamidinyl ligand by the action of CH₃I on complex I. The reaction with CH₃I, followed by the addition of I₂, allowed isolation of [Cp₂V(R(CH₃)NC=NR)]I₃ (II) (R = *p*-CH₃C₆H₄; ν_{CN}(Nujol) 1680 cm⁻¹; μ_{eff} = 1.78 μ_B at 293 K). The X-ray analysis showed an overall structure of the cation similar to that of I, with the amidinyl ligand acting as a three-electron-donor ligand and displaying a bonding mode similar to that observed for η^2-C,O acyls and η^2-C,N iminoacyls. The two C–N bond distances within the CN₂ unit have a high double-bond character (1.26 (2) and 1.33 (2) Å), indicating a significant electronic delocalization all over the VCN₂ unit with a carbenoid character for the carbon bonded to the vanadium atom. In both complexes, V–C bond distances (about 2.0 Å) fall in the expected range for a V–C (sp²) bond. Crystallographic details for complex I: space group *Pna*2₁ (orthorhombic); *a* = 14.446 (3) Å, *b* = 14.186 (2) Å, *c* = 20.903 (4) Å, *V* = 4283.7 Å³; *Z* = 8; D_{calcd} = 1.251 g cm⁻³. The final *R* factor was 8.4% for 1439 observed reflections. Crystallographic details for complex II: space group *P*2₁/*c* (monoclinic); *a* = 14.260 (6) Å, *b* = 19.176 (5) Å, *c* = 10.628 (4) Å; β = 106.92 (5)°; *V* = 2780.4 Å³; *Z* = 4; D_{calcd} = 1.910 g cm⁻³. The final *R* factor was 6.3% for 2283 observed reflections.

Introduction

The interest in carbodiimide–transition metal chemistry is justified by the nature of carbodiimides, which closely imitate carbon dioxide, as well as by the possibility of modifying their reactivity[1] with the assistance of a metal center.
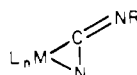
The so far reported results concerning the reaction between carbodiimides and transition-metal complexes have been summarized below.

(i) Carbodiimides have been found to be σ bonded through a nitrogen atom to the metal
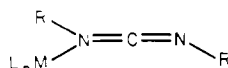
in some Pd(II) complexes.[2]

(ii) Carbene-like metals add to one of the C=N bonds, as in

This metal–carbodiimide interaction suggested for

(PPh₃)₂Ni(PhN=C=NPh)[3] was structurally proven in Cp₂V(*p*-TCD) (Cp = η^5-C₅H₅; *p*-TCD = *p*-tolylcarbodiimide), whose synthesis and structure are described in this paper. This is the first structural report on a metal–carbodiimide complex.

(iii) Metal–carbonyl complexes promote the so-called disproportionation of carbodiimides[4–6] to dihydrotrialkylguanidinium dianion, A, being complexed by the metal and

$$2RN=C=NR + 2e^- \longrightarrow \left[RN-\overset{\overset{\displaystyle NR}{\|}}{C}-NR \right]^{2-} + RNC$$

A
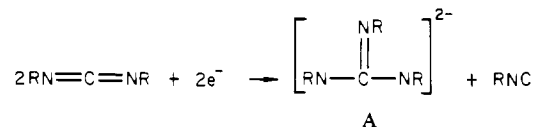
isocyanide. This metal-promoted carbodiimide transformation seems to involve the dimerization of the organic molecule as a key step in a sequence like[6–9]

(1) Reichen, W. *Chem. Rev.* **1978**, *78*, 569.
(2) Bycroft, B. M.; Cotton, J. D. *J. Chem. Soc., Dalton Trans.* **1973**, 1867.
(3) Hoberg, H.; Korff, J. *J. Organomet. Chem.* **1978**, *150*, C20.
(4) Bremer, N. J.; Cutcliffe, A. B.; Farona, M. F.; Kofron, W. G. *J. Chem. Soc. A* **1971**, 3264.
(5) Cotton, J. D.; Zornig, S. D. *Inorg. Chim. Acta* **1977**, *25*, L133.
(6) Duggan, M. D. *Inorg. Chem.* **1979**, *18*, 903.

*To whom correspondence should be addressed at the Università di Pisa.